PROCEEDINGS OF SPIE

SPIEDigitalLibrary.org/conference-proceedings-of-spie

Generation Of Synthetic Aperture Radar Images Using Acousto-Optics

Psaltis, Demetri, Wagner, Kelvin

Demetri Psaltis, Kelvin Wagner, "Generation Of Synthetic Aperture Radar Images Using Acousto-Optics," Proc. SPIE 0271, Advances in Display Technology II, (28 July 1981); doi: 10.1117/12.931763

SPIE.

Event: 1981 Los Angeles Technical Symposium, 1980, Los Angeles, United States

Generation of synthetic aperture radar images using acousto-optics

Demetri Psaltis, Kelvin Wagner
California Institute of Technology, Department of Electrical Engineering, Pasadena, California 91125

Abstract

The applicability of Synthetic Aperture Radar (SAR) imaging to many practical problems is severely limited by the excessive computational load associated with the technique. In this paper we describe a simple real-time, SAR processor which is implemented with acousto-optic and charge-coupled devices. This device will be useful in applications where real-time image formation is essential and in applications where present processors are not cost effective. It could also be used to preview large sets of imagery. The device is very compact and hence it has the potential to operate aboard the vehicle that collects the SAR data.

Introduction

In a conventional imaging system, the resolution of the image is inversely proportional to the size of the aperture of the system.[1] Synthetic Aperture Radar (SAR)[2,3] is a technique by which images with fine resolution can be produced using a small detector aperture. In the SAR system, high resolution is obtained by synthesizing an effective large aperture that does not physically exist. Figure 1 is a schematic diagram of the typical SAR data collection arrangement. The aircraft shown flies with a constant velocity and in a fixed direction parallel to the surface of the earth. A small antenna is mounted on the aircraft. The radiation pattern of this antenna is made to be as wide as possible along the direction of the flight of the aircraft in order to illuminate (and receive backscattered radiation from) a large distance along the ground. As the aircraft travels along x in Figure 1, linearly frequency modulated radio pulses are emitted periodically. For the purposes of this discussion it is convenient to think of the reflectivity of the ground as a weighted distribution of an infinite number of discrete point scatterers. Each pulse is backscattered by point scatterers on the ground and received by the antenna. The round trip delay of each pulse is approximately proportional to the distance y_o in Figure 1.

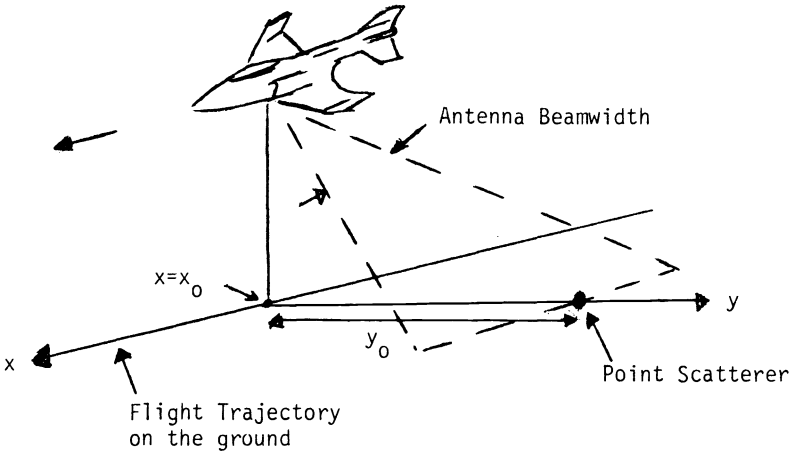

Figure 1. Synthetic aperture radar system

Thus, the location of a point scatterer in the y direction (range) is estimated by measuring the time of arrival of the pulses using pulse compression techniques.[4] The resolution in the y direction is determined by the width of the compressed pulse which is equal to the inverse of the temporal bandwidth of the radar.

As the plane travels, the relative radial velocity between the moving antenna and a stationary point scatterer on the ground changes. Thus, radar pulses received by the antenna from the same point scatterer at different positions (and times) along the path of the aircraft are Doppler shifted by different amounts. The position of the point scatterers

along the x dimension is estimated by detecting the "Doppler history" of the received radar pulses. The resolution in the x direction is inversely proportional to the number of radar pulses that are used in the direction of the Doppler history of a single point scatterer. In a practical system the azimuth resolution is limited primarily by transmitter power limitations. The ability of the SAR system to perform imaging that is essentially independent of the physical size of the aperture of the imaging system is accomplished at the expense of increased complexity in the post-detection processor. In a conventional imaging system, the detected signal is the image itself or at least the image can be readily obtained (in the case of phased antenna arrays). In an SAR system however, the detected signals must be extensively processed to produce the actual image. The transmitted linear FM pulse, s(t), is the form

$$s(t) = a(t)e^{j[\omega_o t + \alpha t^2]} \tag{1}$$

The signal received by the antenna from a single scatterer located at coordinates (x_o, y_o) on the ground can be thought of as a two-dimensional data set. One of the dimensions, η, corresponds to the time history of each received pulse. The second dimension, ξ, is created by the different pulses of the radar. It can be shown[3] that the received signal in this two-dimensional space can be approximated by

$$f(\xi,\eta) \simeq b(\xi,\eta)e^{j\left[\frac{k_1}{y_o}(\xi - x_o)^2 + k_2(\eta - y_o)^2\right]} \tag{2}$$

k_1 and k_2 are constants and $b(\xi,\eta)$ is a slow varying function whose shape is determined by the envelope of the transmitted pulse, a(t), and the diffraction pattern of the antenna. The signal $f(\xi,\eta)$ must be processed to produce an image g(x,y) of the point scatterer:

$$g(x,y) = \int\int f(\xi,\eta)\, h^*(\xi + x, \eta - y)\, d\xi d\eta \tag{3}$$

where $h(\xi,\eta) = e^{j\left[\frac{k_1}{y_o}\xi^2 + k_2\eta^2\right]}$. Equation (3) can be rewritten as follows:

$$g(x,y) = e^{j\left[\frac{k_1}{y_o}(x_o^2 - x^2) + k_2(y_o^2 - y^2)\right]} \times \int\int b(\xi,\eta)e^{-j\left[\frac{k_1}{y_o}(x - x_o)\xi + k_2(y - y_o)\eta\right]} d\xi d\eta$$

$$= e^{j\left[\frac{k_1}{y_o}(x_o^2 - x^2) + k_2(y_o^2 - y^2)\right]} B\left[\frac{k_1}{y_o}(x - x_o), k_2(y - y_o)\right], \tag{4}$$

where $B(\omega_\xi,\omega_\eta)$ is the two-dimensional Fourier transform of $b(\xi,\eta)$. Since $b(\xi,\eta)$ is a slow varying function, its Fourier transform approaches an impulse in the frequency domain. Thus, the image g(x,y) as it is given by Equation (4) is approximately proportional to an impulse centered at $(x = x_o, y = y_o)$ which resembles the original object (the point scatterer).

The computational complexity of SAR image formation is evidenced by Equation (3). In practice approximately 10^5-10^6 complex multiplication and the same number of additions must be performed to obtain an image of a single point scatterer. The parallel processing capability of optical computers can be used to handle this heavy computational load. Indeed, optical computers have been used to process SAR signals since the original inception of the technique.[3,5] In recent years, advances in digital technology have made it possible for digital computers to process SAR signals.[6] However, the present implementations of both digital and optical SAR processors are not suitable for applications in which the SAR images must be formed in real-time. The need for such a capability exists in military applications as well as in the space and earth resources exploration programs. The processor that will be described in the next section is a relatively simple system that has real-time processing capability and the potential for producing SAR images of good quality. Thus, it appears to be most suitable for real-time, on-board processing applications.

Description of the processor

The SAR image, g(x,y) is obtained by performing the two-dimensional correlation described by Equation (3). Since the kernel h(ξ,η) in Equation (3) is separable in ξ and η, Equation (3) can be decomposed into a cascade of an array of one-dimensional correlations in η followed by an array of one-dimensional correlations in ξ.

$$g(x,y) = \iint f(\xi,\eta)\, e^{-j\left[\frac{k_1}{y_o}(\xi - x)^2 + k_2 (\eta - y)^2\right]} d\xi d\eta$$

$$= \int \left[\int f(\xi,\eta) e^{-jk_2(\eta - y)^2} d\eta\right] e^{-j\frac{k_2}{y_o}(\xi - x)^2} d\xi. \qquad (5)$$

Remember that the variation of $f(\xi,\eta)$ in η corresponds to the time history of the back-scattered pulses, while ξ corresponds to the index of the pulses arriving consecutively at the antenna. Equation (5) can therefore be implemented by a single fast one-dimensional correlator in the η direction that computes the correlation for different ξ values (pulses) consecutively. The output of this correlator can then be processed by an array of slow one-dimensional correlators in ξ operating in parallel. In our system an Acousto-Optic (AO) correlator[7] will perform the fast correlation. A Charge-Coupled Device (CCD) detector array[8] will serve as the array of slow correlators.[9]

The system is shown in Figure 2a. It consists of an AO device, a single lens and a CCD detector array. The signal, $S_R(t)$, received by the antenna of the SAR system is heterdyned to the center frequency of the piezoelectric transducer and then applied to the AO device. For weak modulation, the amplitude of the light diffracted to the first order is proportional to $S_R(t - \frac{x}{v})$,[10] where x is the spatial dimension along the direction of acoustic wave propagation, and v is the speed of sound. At periodic time instances the spatial modulation in the device corresponds to the backscattered signal from a single radar pulse. At these instances, the illuminating laser is pulsed. For a single point scatterer, the amplitude of the light diffracted by the AO device during each laser pulse is proportional to the function in Equation (2) for a fixed value of the parameter ξ (the pulse number). A single lens is used to bring this light field into focus to form the image of the point scatterer in the range direction (Figure 2b). The focusing action of the lens is the equivalent of performing the integration over η in Equation (5). Each range compressed signal is detected by the CCD array and each pixel in the horizontal direction corresponds to a different range cell. Imaging in the azimuth direction is accomplished by the CCD array which is used not only as the detector but also simultaneously as a time integrating correlator array. A light modulating mask is placed in front of the CCD. The transmittance of this mask in the vertical direction is a linear frequency modulated signal and the modulation level increases linearly in the horizontal direction. In other words, the transmittance of the mask corresponds to the portion of the kernel in Equation (5) that depends on ξ. The signal detected by the CCD array each time the source is pulsed is the product of the return signal from each radar pulse, compressed in range, and the transmittance of the mask. While the return signal from the next radar pulse is entering the acousto-optic device (.1-2 msec), the charge pattern stored in the CCD is shifted vertically by one pixel. When the light source is pulsed again, the CCD array detects the light corresponding to the second range compressed radar pulse and adds it to the already stored, but vertically shifted, signal from the previous radar pulse. This is repeated for N radar pulses (where N is the number of pixels of the CCD in the vertical direction). The signal that is eventually read out at each range cell is the correlation of the transmittance of the mask at each range position and the variation of the range compressed signal as a function of radar pulse number, ξ. This is the desired azimuth imaging operation as described in Equation (5). As the range and azimuth compressed signals reach the lower end of the CCD array in Figure 2, they are transferred to the horizontal CCD shift register and they are quickly read out. The azimuth slices are continuously produced as long as the flight continues.

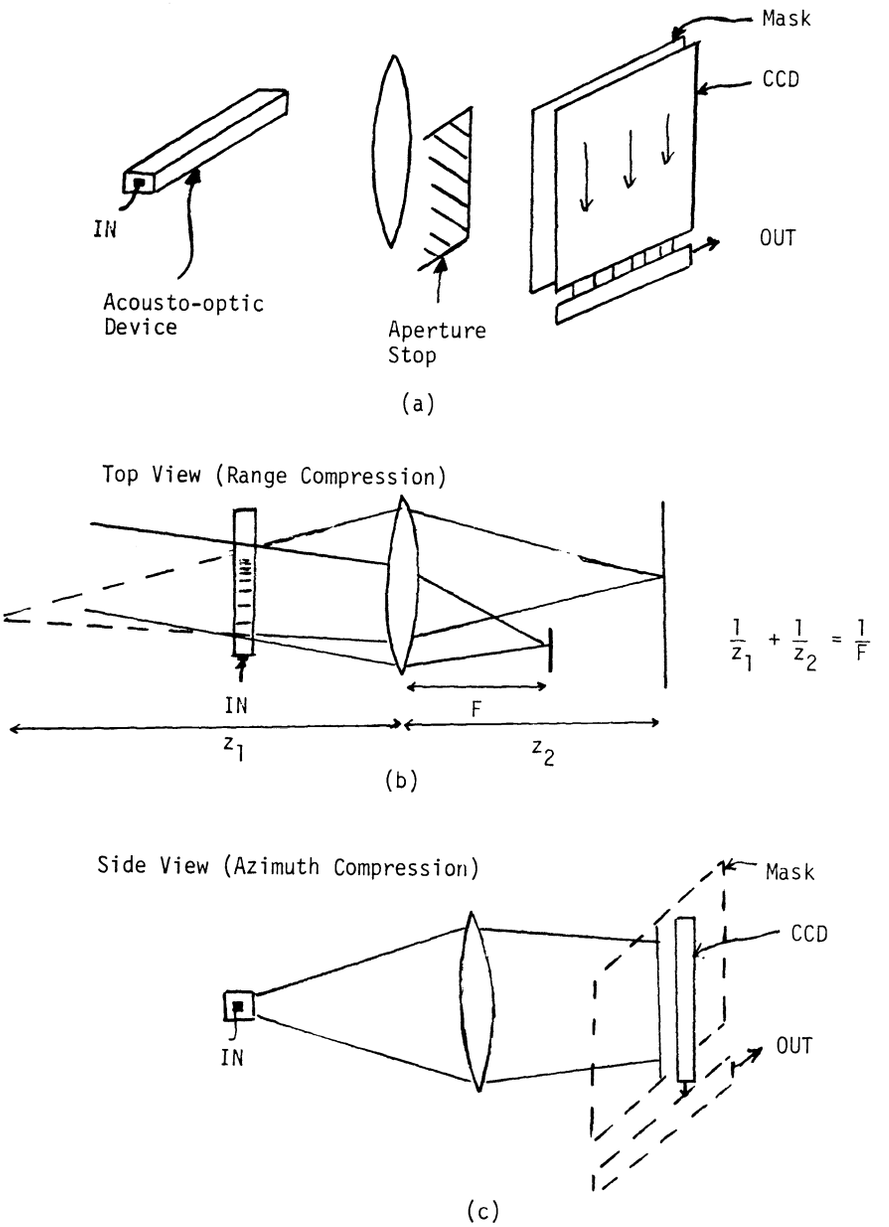

Figure 2. Acousto-optic/CCD synthetic aperture radar processor

Performance characteristics

In Table 1 we list some of the relevant performance characteristics of the acousto-optic/CCD SAR processor. Two sets of characteristics are considered. The first set is for the experimental processor that we are presently constructing. The specification for this processor will be matched to the radars now in use at the Jet Propulsion Laboratory (JPL), since we intend to use their data for testing. The experimental processor uses a 512 x 320 CCD imaging array and an AO cell with 40 MHz bandwidth and 10 μsec aperture. This system is not yet operational and the performance characteristics listed in Table 1 are calculated rather than measured. The second set of characteristics is the optimum performance attainable with state-of-the-art components. The resolution in range is given by[2]

$$\rho_R = \frac{C}{2B} \tag{6}$$

where C is the speed of light and B is the bandwidth of the transmitted chirp signal. To attain this resolution the bandwidth of the AO cell must also be equal to B. For B = 40 MHz, $\rho_A \approx 4$m. AO devices with bandwidths of more than 1 GHz[12] are available, hence the maximum range resolution is not limited by the AO device. The pulse duration of the light

Table 1. Performance characteristics of the AO/CCD SAR camera

	LIMITING FACTOR	EXPERIMENTAL PROCESSOR	MAXIMUM POSSIBLE
RANGE RESOLUTION $\rho_R = \frac{C}{2B}$	AO Bandwidth Light pulse duration Range curvature	$\rho_R \simeq 10\text{-}20m$	$\rho_R < 1m$
NUMBER OF RANGE RESOLUTION ELEMENTS	-Size of the CCD array in the non-shift direction. -AO aperture.	160 or 320	1200
AZIMUTH RESULTION $\rho_A = \frac{L}{N}$	-Size of the CCD array in the shift direction. -Mask -Temporal stability	N = 512 or 256 $\rho_A \simeq 30\text{-}60m$	$\rho_A \sim 15m$
NUMBER OF AZIMUTH RESOLUTION ELEMENTS	Not limited by the processor.		
IMAGE QUALITY Dynamic range SNR Geometric registration	-CCD Detector noise Dynamic range Blooming -AO Linearity Amplifier noise -Optics	Dynamic Range 250-300 : 1	Dynamic Range 500 : 1

source has to be several times shorter than 1/B to avoid blurring of the SAR image as it is detected by the CCD. Mode locked argon lasers produce pulses with duration 200-300 psec. The resolution in range can be also degraded by the spatial response of the system (the MTF of the imaging system and the CCD array). Finally, the resolution is ultimately limited by the range curvature[11] (the slight variation of the range as a function of azimuth). For the JPL radars and within the limitations of our experimental processor, the range curvature is not a factor.

The number of resolution cells in the range direction is limited by the size of the CCD array in the non-shifting (horizontal in Figure 2) dimension and the time-bandwidth product of the AO device. The range compressed signals must be detected coherently (amplitude and phase detection). Coherent detection is accomplished by introducing a spatial carrier in the SAR image in either the range or azimuth direction. If the carrier is introduced in range the maximum number of range cells is one half of the horizontal size of the CCD array.

The resolution in azimuth can be expressed as

$$\rho_A = \frac{L}{N} \tag{7}$$

where L is the distance on the ground along the cross range (azimuth) direction, illuminated by the main lobe of the antenna pattern and N is the number of radar pulses that are integrated to form the SAR image. L is determined by the geometry of the radar. N is limited by the size of the CCD array in the shifting (vertical) direction. For the JPL radar and the CCD we are using, L ≃ 15000m, and ρ_A = 15000/512 ≃ 30m. If the spatial carrier is introduced in the azimuth direction, ρ_A is doubled. The azimuth resolution may be further degraded by our inability to fabricate the optical mask in Figure 2 to exact specification, spatial variations in the illuminating light beam and temporal instability of the electronics in the system.

In Table 1 we include in the term "image quality" all the factors affecting the fidelity with which images of the ground reflectivity are reproduced. Sources of degradation in image quality can be classified as either deterministic or random. Deterministic degradations can occur because of aberrations in the optical system, non-linearity of the AO deflector, and pixel-to-pixel variation in the responsivity of the CCD array (fixed pattern noise). In principle, the majority of these degradations can be removed by careful engineering and post-detection processing. Random degradations occur in the processor because of amplifier (thermal) noise in the circuit that drives the AO device, optical noise (speckle and scattered light) and detector noise. The most critical measure of image quality (except for resolution) is the linear dynamic range in the image, defined as

the maximum signal value divided by the minimum detectable variation in the signal (sensitivity). We estimate that the CCD array will be the primary factor limiting the dynamic range of the SAR images.[12] The array we are using has a full-well capacity (maximum signal) of 250,000 electrons, with excellent linearity in this range. Since the images are detected on a bias, the maximum signal is only 125,000 electrons. The sensitivity is determined by thermal noise due to on- and off-chip amplifiers in the detector, switching noise that arises from transients in the clock waveforms that control the data transfer in the CCD and quantum noise. A large portion of the detector noise is concentrated at low frequencies and it can be removed by appropriate filtering. In our system, we use double-correlated-sampling[13] which reduces the dark level signal to 200e per pixel at room temperature. The quantum noise due to the bias is $\sqrt{125,000} \simeq 350$ electrons. At low signal levels the sensitivity of the detector is 350+200 = 550 electrons. The approximate dynamic range is equal to 125000/550. The dynamic range can be improved by cooling the detector and reducing the bias (and signal) level.

Acknowledgement

The authors thank Thomas Bicknell of the Jet Propulsion Laboratory for contributing the CCD camera and a lot of his time to this project.

References

1. J. W. Goodman, "Introduction to Fourier Optics", McGraw-Hill, New York, 1968.
2. W. M. Brown, "Synthetic Aperture Radar", IEEE Trans. Aerospace and Electronic Systems AES-3, 217-229 (1967).
3. L. J. Cutrona, et al, "On the Application of Coherent Optical Processing Techniques to Synthetic Aperture Radar", Proc. IEEE, 54, 1026 (1966).
4. M. I. Skolnik, "Introduction to Radar Systems", Chapter 10, McGraw-Hill, New York, 1962.
5. K. Preston, "Coherent Optical Computers", McGraw-Hill, New York, 1972.
6. J. C. Kirk, "A Discussion of Digital Processing in Synthetic Aperture Radar", IEEE Trans. Aerospace and Electronic Systems, AES-11(3), 326-337 (1975).
7. I. C. Chang, "Acousto-optic Devices and Applications", IEEE Trans. Sonics and Ultrasonics, SU-23(1), 2-22 (1976).
8. D. F. Barbe, "Imaging Devices Using the Charge-Coupled Device Concept", Proc. IEEE, 63, 38-67 (1975).
9. M. A. Monahan, et al, "Incoherent Electro-Optical Processing with CCD's", Digest of the International Optical Computing Conference, Washington, D. C., 1975. (IEEE Catalog 75 C40941-5C)
10. R. A. Sprague, "A Review of Acousto-optic Signal Correlators", Optical Engineering, 16-5, 467 (1977).
11. E. N. Leith, "Range-Azimuth-Coupling Aberrations in Pulse-Scanned Imaging Systems", J. Opt. Soc. Am., 63(2), 119 (1973).
12. G. M. Borsuk, "Photodectors for Acousto-optic Signal Processors", Proc. IEEE, 69(1), 100 (1981).
13. J. A. Hall, "Arrays and Charge-Coupled Devices", Chapter 8 in "Applied Optics and Optical Engineering", Volume VIII, edited by R. Shannon and J. Wyant, Academic Press, 1980.